Ridgelet Transform Based on Reveillès Discrete Lines

Philippe Carré and Eric Andres

Laboratoire IRCOM-SIC,
bât. SP2MI, av. Marie et Pierre Curie
BP 30179 - 86960 Chasseneuil-Futuroscope Cédex - FRANCE

Abstract. In this paper we present a new discrete implementation of ridgelet transforms based on Reveillès discrete 2D lines. Ridgelet transforms are particular invertible wavelet transforms. Our approach uses the arithmetical thickness parameter of Reveillès lines to adapt the Ridgelet transform to specific applications. We illustrate this with a denoising and a compression algorithm. The broader aim of this paper is to show how results of discrete analytical geometry can be sucessfully used in image analysis.

1 Introduction

Image analysis is traditionally aimed at understanding digital signals obtained by sensors (in our case cameras). Digital information is considered as sampled continuous information and the theoretical background for it is signal theory. This is sometimes referred to as *"digital geometry"* in opposition to *"discrete geometry"* for computer graphics. These last ten years, since J-P. Reveillès has introduced it [1], *discrete analytical geometry* has made an important progress in defining and studying classes of discrete objects and transformations. This greatly enhanced our understanding of the links between the discrete world $\mathbb{Z}^n$ and the continuous world $\mathbb{R}^n$. In the same time, a new discrete signal decomposition has been developed in image analysis: the wavelet representation. This new representation has many applications such as denoising, compression, analysis, etc. One of the aims of this paper is to apply this new insight in discrete geometry to image analysis and more specifically to a particular wavelet transform: the ridgelet transform.

Wavelets are very good at representing point singularities ; however they are significantly less efficient when it comes to linear singularities. Because edges are a extremely common phenomena in natural images, an efficient multiresolution representation of images with edges would be quite advantageous in a number of applications. A team of Stanford has recently developed an alternative system of multiresolution analysis specifically designed to efficiently represent edges in images [2]. Their attempt was to design a new system, called ridgelet transform, in the continuous domain so that an image could be approximated within a certain margin error with significantly fewer coefficients than would be required

A. Braquelaire, J.-O. Lachaud, and A. Vialard (Eds.): DGCI 2002, LNCS 2301, pp. 417–427, 2002.

after a wavelet decomposition. However, most of the work done with ridgelets has been theoretical in nature and discussed in the context of continuous functions. The important bridge to digital implementation is tenuous at best. To our knowledge, we can find in the literature only two solutions for the digital ridgelet decomposition [3], [4] (notice that the study proposed by Guédon et al is similar [5]).This paper presents a new approach that aims at representing linear singularities with a discrete ridgelet transform based on Reveillès discrete lines.

In this article, we propose a new approach of the ridgelet transform based on several types of Reveillès discrete lines definitions in the Fourier domain. Our decomposition has an exact inverse reconstruction process and the redundancy of our Ridgelet representation can be adjusted with the arithmetical thickness of the Reveilles discrete lines. To illustrate this new decomposition, we propose a method of restoration of noised images which uses a wavelet undecimated method defined in [6].

2 The Ridgelet Transform

2.1 The Wavelet Transform

The discrete wavelet transform (DWT) stems from the multiresolution analysis and filter bank theory [7]. The multiresolution analysis is a decreasing sequence of closed subspace $\{V_j\}_{j\in Z}$ that approximates $L^2(\Re)$ ($f \in L^2(\Re)$ if $\int_{-\infty}^{\infty} \|f(x)\|^2 dx < \infty$). A function $s \in L^2(\Re)$ is projected, at each step l, onto the subset V_l. This projection is defined as the scalar product, noted c_l, of s with a scaling function, noted ϕ that is dilated and translated:

$$c_l(k) = \left\langle s(x), 2^{-l/2}\phi\left(2^{-l}x - k\right)\right\rangle = \langle s(x), \phi_{l,k}(x)\rangle \tag{1}$$

k is the translation parameter and l is the dilatation parameter with $k, l \in Z$.

At each step (if l is growing), the signal is smoothed. The lost informations can be restored using the complementary subspace W_{l+1} of V_{l+1} in V_l. This subspace is generated by a wavelet function ψ with integer translation and dyadic dilatation; the projection of s on W_l is defined as the scalar product, noted d_l:

$$d_l(k) = \left\langle s(x), 2^{-l/2}\psi\left(2^{-l}x - k\right)\right\rangle = \langle s(x), \psi_{l,k}(x)\rangle \tag{2}$$

Then, the analysis is defined as :

$$c_l(k) = \frac{1}{\sqrt{2}}\sum_n h(n-2k)c_{l-1}(k),\ d_l(k) = \frac{1}{\sqrt{2}}\sum_n g(n-2k)c_{l-1}(k)$$

with c_l the coarse approximation, d_l the decimated wavelet coefficients at scale l and c_0 the original signal, the sequence $\{h(k), k \in Z\}$ is the impulse response

of a low-pass filter and the sequence $\{g(k), k \in Z\}$ is the impulse response of a high-pass filter. Notice that with conditions required on the filters, we get an exact restoration.

Mallat's multiresolution analysis is connected with so called "pyramidal" algorithms in image processing [8]. Because of decimation after filtering, the Mallat's decomposition is completely time variant. A way to obtain a time-invariant system is to compute all the integer shifts of the signal. Since the decomposition is not decimated, filters are dilated between each projection. This algorithm presents many advantages, particularly a knowledge of all wavelets' coefficients: coefficients removed during the downsampling are not necessary for a perfect reconstruction, but they may contain information useful for the denoising.

2.2 Continuous Theory of Ridgelet Transform

A substantial foundation for Ridgelet analysis is documented in the Ph.D. thesis of Candès [2]. We briefly review the ridgelet transform and illustrate its connections with the radon and wavelet transforms in the continuous domain. The continuous ridgelet transform of $s \in L^2\left(\Re^2\right)$ is defined by :

$$r(a,b,\theta) = \int_{R^2} \psi_{a,b,\theta}(\mathbf{x}) s(\mathbf{x}) d\mathbf{x}$$

with $\psi_{a,b,\theta}(\mathbf{x})$ the ridgelet 2-D function defined from a wavelet 1-D function ψ as:

$$\psi_{a,b,\theta}(\mathbf{x}) = a^{-1/2}\psi\left(\frac{x_1\cos\theta + x_2\sin\theta - b}{a}\right)$$

b is the translation parameter, a is the dilatation parameter and θ is the direction parameter.

The function is oriented at the angle θ and is constant along lines $x_1\cos\theta + x_2\sin\theta = cst$. Transverse to these ridges it is a wavelet. In comparison, the analysis continuous 2-D wavelet function are tensor products of 1-D wavelet $\psi_{a,b}$:

$$\psi_{\mathbf{a},\mathbf{b}}(\mathbf{x}) = \psi_{a_1,b_1}(x_1)\psi_{a_2,b_2}(x_2)$$

The Radon transform seems to be similar to the 2-D wavelet transform but the translation parameters (b_1, b_2) are replaced by the line parameters (b, θ). Then, the wavelets are adapted to analyse isolated point discontinuities, while the ridgelets are adapted to analyse discontinuities along lines.

A basic tool for calculating ridgelet coefficients is to view ridgelet analysis as a form of wavelet analysis in the Radon domain: in 2-D, points and lines are related via the radon transform, thus the wavelet and ridgelet transforms are linked via the Radon transform.

The Radon transform of s is defined as:

$$Rs(\theta,t) = \int_{R^2} s(\mathbf{x})\delta(x_1\cos\theta + x_2\sin\theta - t)dx_1dx_2$$

where δ is the Dirac distribution. The ridgelet coefficients $r(a, b, \theta)$ of s are given by the 1-D wavelet transform to the projections of the Radon transform where the direction θ is constant and x is varying:

$$r(a, b, \theta) = \int_R \psi_{a,b}(x) Rs(\theta, x) dx$$

Notice that the Radon transform can be obtained by applying the 1-D inverse Fourier transform to the 2-D Fourier transform restricted to radial lines going through the origin (this is exactly what we are going to do in the discrete Fourier domain with help of discrete Reveillès lines):

$$\widehat{s}(\omega \cos\theta, \omega \sin\theta) = \int_R e^{-j\omega x} Rs(\theta, x) dx$$

with $\widehat{s}(\omega)$ the 2-D Fourier transform of s.

This is the projection-slice formula which is used in image reconstruction from projection methods. We deduce that the Radon transform can be obtained by applying the 1-D inverse Fourier transform to the 2-D Fourier transform restricted to radial lines going through the origin. These relations are shown in figure 1.

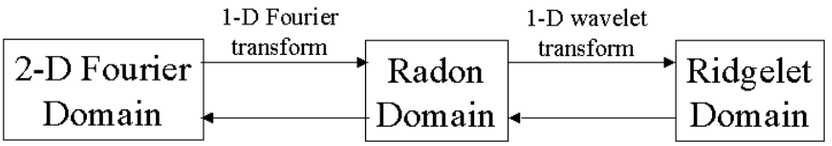

Fig. 1. Relation between transforms

2.3 Discrete Ridgelet Transform

As we have seen, a basic strategy for calculating the continuous ridgelet transform is first to compute the Radon transform $Rs(\theta, t)$ and secondly, to apply a 1-D wavelet transform to the slices $Rs(\theta, .)$. The discrete procedure uses the same principle.

As presented in the first section, the discrete wavelet decomposition is easy to implement, is stable and invertible, and can be associated to a discrete orthogonal representation.

The discretization of the Radon transform is more difficult to achieve. The majority of methods proposed in the literature have been devised to approximate the continuous formula. But, none of them were specifically designed to be invertible transforms for discrete images and can not be used for the discrete

Ridgelet transform. Recently, some articles studied the implementation of the digital Ridgelet transform. Two approaches have been developed:

- Spatial strategy for digital Radon transform: the Radon transform is defined as summations of image pixels over a certain set of lines. Those lines are defined in a finite geometry in a similar way as the line for the continuous Radon transform in the Euclidean geometry.

  $$Rs(p,q,b) = \sum_x \sum_y s(x,y)\delta\left(b + px - qy\right) \text{ with } (p,q) \text{ direction of projection}$$

  In [5] an inverse transform based on erosion and dilatation operations is proposed. Vetterli et al. proposed in [3] an orthonormal ridgelet transform.
- Fourier strategy for digital Radon transform: the projection-slice formula suggests that approximate Radon transforms for digital data can be based on discrete Fast Fourier transforms (FFT). This is a widely used approach in the literature of medical imaging and synthetic aperture radar imaging. The Fourier-domain computation of an approximate digital radon transform is defined as:
  1. Compute the 2-D FFT of f
  2. Extract Fourier coefficients which fall lines L_θ going through the origin.
  3. Compute the 1-D FFT on each line L_θ (defined for each value of the angular parameter).

  In this strategy too, discrete lines must be defined. In [4], Starck et Al proposed to use an interpolation scheme which substitutes the sampled value of the Fourier transform obtained on the square lattice with sampled value of $\widehat{s}$ on a polar lattice. In this paper, we propose to define the lines L_θ with the discrete geometry in the Fourier domain. This solution allows us to have different Ridgelet decompositions according to the arithmetical thickness of the discrete Reveillès lines. Our transformation is redundant but the repetition of information depends on the type of the discrete lines used and can be adapted with the application. Moreover we obtain an exact reconstruction.

3 Digital Radon Transform Based on Reveillès Discrete 2D Lines

3.1 Definition of Discrete Lines

The discrete lines that are used in our application are not classical discrete lines such as, for instance, Bresenham lines nor the classical Reveillès lines. These lines are not suitable for our purpose because they do not provide a central symmetry in the Fourier domain. Without central symmetry, the inverse Fourier transform would produce imaginary values during the Radon transform. Central symmetry is obtained easily by using closed Reveillès discrete lines defined as follows:

$$L^{\omega}_{(p,q)} = \left\{(x,y) \in \mathbb{Z}^2 \,||px + qy| \leq \omega/2\right\}$$

with $(p,q) \in \mathbb{Z}^2$ the direction of the line (direction of Radon projection) and ω the arithmetical thickness.

The parameter ω defines the connectivity of the discrete lines. The closed discrete lines have many interesting properties. One of the most important ones is that each type of closed discrete line is directly linked to a distance: for instance

$$L_{(p,q)}^{\sqrt{p^2+q^2}} = \left\{ (x,y) \in \mathbb{Z}^2 \left| |px+qy| \leq \frac{\sqrt{p^2+q^2}}{2} \right. \right\}$$

is equal to $\left\{ M \in \mathbb{Z}^2 \left| d_2\left(M, \mathcal{L}_{(p,q)}\right) \leq \frac{1}{2} \right. \right\}$ where $\mathcal{L}_{(p,q)} : px + qy = 0$ is the Euclidean line of direction (p,q) and d_2 the Euclidean distance [9].

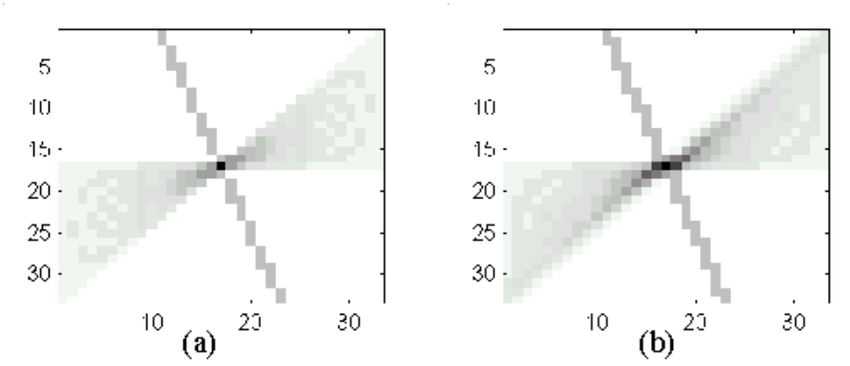

Fig. 2. Redundancy on the cover of the Fourier lattice by (a) closed naïve lines (b) supercover lines

3.2 Closed Reveillès Discrete Lines for Digital Radon Transform

Our Digital Radon transform is defined by:

$$R^{\omega}s(p,q,b) = \sum_{k=0}^{K} \widehat{s}(\mathbf{f}_k) e^{2\pi j \frac{k}{K} b} \text{ with } \mathbf{f}_k = \begin{pmatrix} f_1^k \\ f_2^k \end{pmatrix} \text{ such that } \left| pf_1^k + qf_2^k \right| \leq \omega/2$$
$$\text{and } K \text{ the length of a line segment of } L_{p,q}^{\omega}$$

We must define the set of discrete directions (p,q) in order to provide a complete representation. The set of line segments must cover all the square lattice in Fourier domain. For this, we define the direction (p,q) according to pairs of symmetric points from the boundary of the 2-D Discrete Fourier Spectra.

Proposition 1. *Let a square lattice be defined as* $\Omega_N^2 = [-N, N] \times [-N, N]$. *Let us consider the set of directions* (p_m, q_m) *with, for* $0 \leq m \leq 2N$, $(p_m, q_m) = (N, m - N)$ *and for* $2N + 1 \leq m \leq 4N - 2$, $(p_m, q_m) = (m - 3N + 1, N)$. *The set of all the closed lines defined by* $|p_m f_1 + q_m f_2| \leq \omega_m/2$ *with* $\omega_m \geq \sup(|p_m|, |q_m|)$ *provides a complete cover of the lattice* Ω_N^2.

The proof of this proposition is obvious because of a well known result in discrete analytical geometry that states that a closed discrete line of direction (p, q) is connected if and only if $\omega \geq \sup(|p|, |q|)$ [1]. For thinner (non connected) discrete lines, with values of $\omega < \sup(|p|, |q|)$, it is possible but not certain that we also achieve a complete cover of the lattice Ω_N^2 depending on the value of ω compared to N. However, for our applications, we preferred working with connected discrete lines.

Figure 2 illustrates the cover of the Fourier lattice (on the first octant) by two different types of discrete lines. The grey value of the pixels represents the redundancy in the projection (number of times a pixels belongs to a discrete line). One isolated line is drawn to shown the illustrate the arithmetical thickness of each type of line.

Three different types of closed discrete lines have been tested:

- closed naive discrete lines: $\omega = \sup(|p|, |q|)$. These lines are the thinnest connected closed discrete lines. They are 8-connected. They provide therefore the smallest redundancy as we can see on figure 2(a). Closed naive discrete lines are related to the distance d_1: $L_{(p,q)}^{\sup(|p|,|q|)} = \left\{ M \in \mathbb{Z}^2 \left| d_1\left(M, \mathcal{L}_{(p,q)}\right) \leq \frac{1}{2} \right.\right\}$ where $d_1(A, B) = |x_A - x_B| + |y_A - y_B|$;
- supercover lines: $\omega = |p| + |q|$. These lines are the thickest connected closed discrete lines that have been considered in our applications. They are the thinnest closed lines that are 4-connected and that cover the Euclidean line they approximate. They provide of course an important redundancy as we can see on figure 2(b). Supercover lines are related to the distance d_∞: $L_{(p,q)}^{|p|+|q|} = \left\{ M \in \mathbb{Z}^2 \left| d_\infty\left(M, \mathcal{L}_{(p,q)}\right) \leq \frac{1}{2} \right.\right\}$. The supercover lines have an important theoretical importance.
- closed Pythagorean lines: $\omega = \sqrt{p^2 + q^2}$. These lines are 8-connected and offer a medium redundancy, in between the naive and supercover lines. The lines are related to the Euclidean distance d_2:

$$L_{(p,q)}^{\sqrt{p^2+q^2}} = \left\{ M \in \mathbb{Z}^2 \left| d_2\left(M, \mathcal{L}_{(p,q)}\right) \leq \frac{1}{2} \right.\right\}.$$

  These lines possess the property of having a number of pixels per period close to its length. This means, in practice, that if pixels of the discrete line would hold energy, this energy would be distributed evenly along the line in the same way independently of the slope of the line.

3.3 Discrete Ridgelet Transform

Now, to obtain the Ridgelet transform, we simply apply the 1-D wavelet transform on each discrete Radon coefficients $R^{\omega}s(p,q,b)$ obtained on the line segment $L^{\omega}_{p,q}$.

This transform is easily invertible. The reconstruction procedure works as follows:

1. Compute the inverse 1-D wavelet transform followed by the inverse 1-D FFT transform for each set $R^{\omega}s(p_m,q_m,.)$ with $m \in [0,4N-2]$
2. Substitute the sampled value of $\widehat{f}$ on the lattice where the points fall on lines $L^{\omega}_{p,q}$ with the sampled value of $\widehat{f}$ on the square lattice.

The precedent procedure permits one to obtain an exact reconstruction if the set of $M = 4N-2$ lines provides a complete cover of the square lattice.

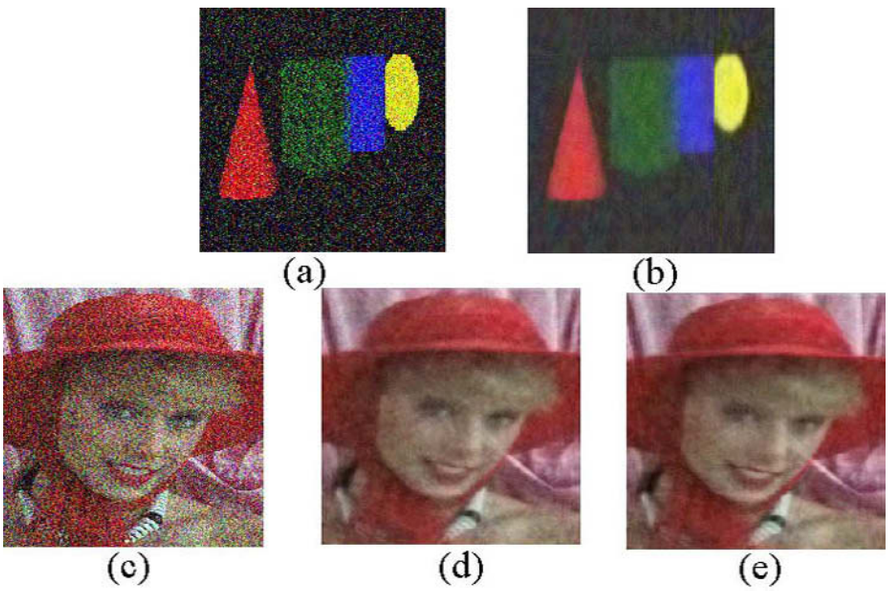

Fig. 3. (a) Noisy image "object" (b) denoised by ridgelet decomposition with pythagoricean discrete lines, $\omega = \sqrt{q^2+p^2}$(c) noisy image woman (d) denoised by ridgelet decomposition with naïve lines, $\omega = \max(|p|,|q|)$ (e) denoised by ridgelet decomposition with supercover lines, $\omega = |p| + |q|$.

Now with our invertible discrete Radon transform, we can obtain an invertible discrete Ridgelet transform by taking the discrete wavelet transform on

each Radon projection sequence $\{R^{\omega}s(p_m, q_m, k)\}_{b\in[0,K-1]}$ where the direction (p_m, q_m) is fixed. This wavelet transform can be decimated or undecimated and the wavelet base can be adapted according to the application, as for the classical wavelet decomposition. Notice that our strategy generalizes and unifies the methods proposed in the litterature that use particular forms of discrete lines (see section on discrete ridgelet transform).

4 Illustration and Discussion

To illustrate the different applications that can be achieved with the new discrete ridgelet transform based on closed Reveillès discrete lines, we have developed two examples: a denoising and a compression algorithm.

The procedure of denoise by Ridgelet transform consists simply in thresholding the Ridgelet coefficients and computing the inverse Ridgelet transform. The thresholding is performed with help of an undecimated method developed for the wavelet decomposition [6]. The redundancy of the wavelet decomposition, associated with this method, reduces artifacts which appear after thresholding [6].

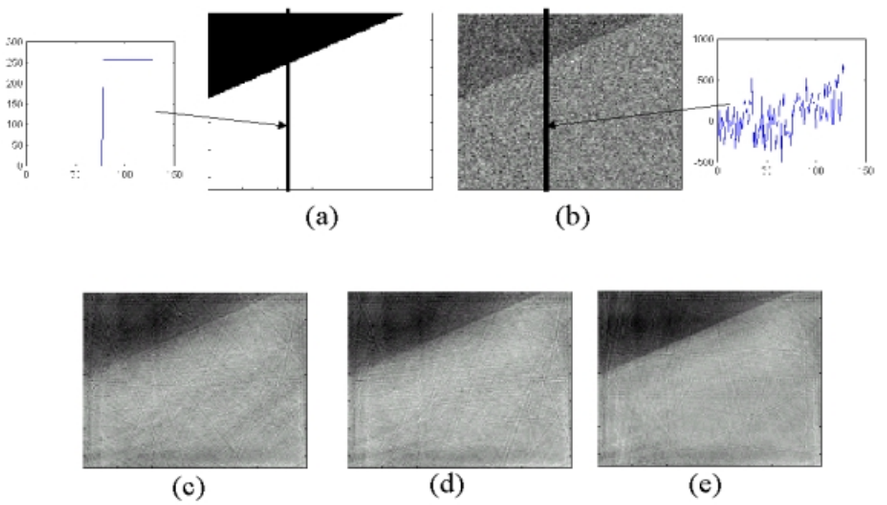

Fig. 4. (a) Original image (b) noisy image (c) denoising with naïve lines (d) denoising with pythagoricean lines (e) denoising with supercover lines

We present in the figure two results of our denoising method. With the first example, we can see that this method can reconstruct very noisy images. Because of the adaptation of this decomposition to linear singularities, the edges of

objects are preserved and the noise seems to be removed. The second example illustrates the results for different definition of the lines $L^{\omega}_{p,q}$. As for the first image, the features are generally correctly reconstructed and the noise is smoothed. But if we study more precisely the result on the woman's hat, we see that the denoising is better for $\omega = |p| + |q|$, supercover lines, than for $\omega = \max(|p|, |q|)$, naive discrete lines. The first choice of arithmetical thickness ω introduces more redundancy into the decomposition. Due to this redundancy we obtain an average value during the reconstruction process that reduces the artifacts.

In order to illustrate more precisely the result of the denoising algorithm with different type of discrete closed lines we have generated an artificial image (Figure 4 (a)) and added important white noise (Figure 4 (b)). To show the effect of the noise we have added a vertical slice of each image (at the left of (a) and right of (b)). Figures 4 (c), (d) and (e) are the results obtained with the denoising algorithm for the three definitions of closed discrete lines. As we can see, for a more redundant decomposition (supercover discrete lines, figure 4 (e)) the denoising is better than for a lesser redundant decomposition (4 (c)).

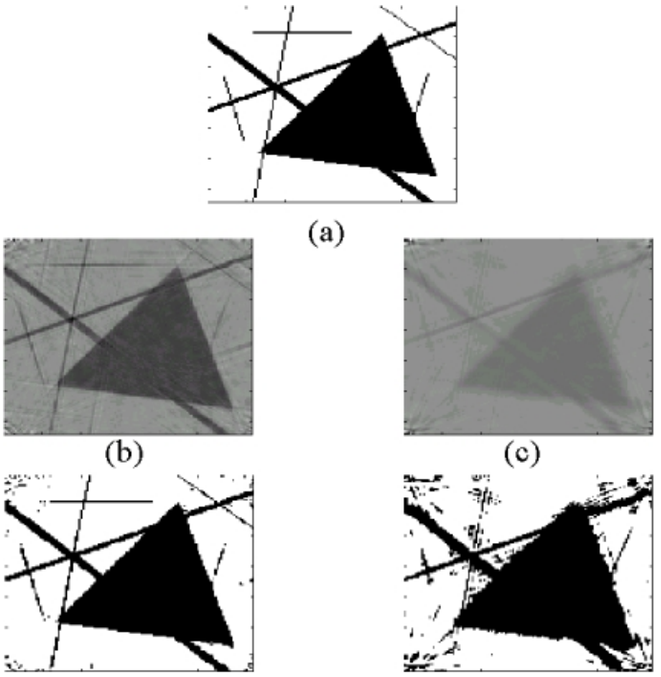

Fig. 5. (a) Original image (b) image compressed at 70% with naïve discrete lines (c) image compressed at 70% with supercover lines

Contrary to the denoising algorithm problematic, for an efficient compression algorithm, redundancy is of course not interesting (more redundancy means more information and thus less compression). In our example, Figure 5, in order to obtain a compression of the image, we have selected in the ridgelet decomposition, the 30% most important (highest) coefficients. This leads to a 70% compression rate. Of course, this is not a very sophisticated procedure and post-processing would be applied in real applications. This illustrates however how the arithmetical thickness of the discrete lines employed in our ridgelet transform influences the quality of the compressed image. As expected, the lower redundancy representation (naive discrete lines) preserves all the features of the original image after thresholding (Figure 5 (b)). On the other hand, with the higher redundancy representation (supercover lines) we loose features and the image is globally of lower quality.

This work can be extended in several directions. One of the more theoretical discrete geometry question that is the question of the smallest value of ω for which we one could obtain a full cover of the Fourier lattice. This is still an open and it seems difficult arithmetical problem. We are also considering extending our denoising and compression algorithms with more sophisticated filters and parameters. It is clear that, for instance, the quality of the result of compression algorithm, where we have performed a simple thresholding, can be increased.

References

1. Reveillès, J.P.: Géométrie discrète, calcul en nombres entiers et algorithmique. Habilitation, Université Louis Pasteur de Strasbourg (1991)
2. Candès, E.: Ridgelets: Theory and Applications. PhD thesis, Stanford (1998)
3. Do, M., Vetterli, M.: Discrete ridgelet transforms for image representation. Submitted to IEEE Trans. on Image Processing (2001)
4. Starck, J.L., Candès, E.J., Donoho, D.L.: The curvelet transform for image denoising. Technical report, Department of Statistics, Stanford (2000)
5. Normand, N., Guedon, P.: Transformee mojette : une transformee redondante pour l'image. Compte rendu de l'Académie des Sciences (1998)
6. Carré, P., Leman, H., Marque, C., Fernandez, C.: Denoising the EHG signal with an undecimated wavelet transform. IEEE Trans. on Biomedical Engineering **45** (1998) 1104–1113
7. Mallat, S.: A theory for multiresolution signal decomposition: the wavelet transform. IEEE Trans. on PAMI **11** (1989) 674–693
8. Burt, P., Adelson, E.: The laplacien pyramid as a compact image code. IEEE Trans. Comm. **31** (1983) 482–550
9. Andrès, E.: Modélisation analytique discrète d'objets géométriques. Habilitation, Université de Poitiers (2000)